



2 Comparison and validation of eight satellite rainfall products over the 3 rugged topography of Tekeze-Atbara Basin at different spatial and 4 temporal scales

6 Tesfay G. Gebremicael^{1,2,3}, Yasir A. Mohamed^{1,2,4}, Pieter van der Zaag^{1,2} Amdom G.
Berhe⁵, Gebremedhin G. Haile³, Eyasu Y. Hagos⁵, Mulubrhan K. Hagos³

8 ¹IHE Delft Institute for Water Education, P.O. Box 3015, 2601 DA Delft, The Netherlands

10 ²Delft University of Technology, P.O. Box 5048, 2600 GA Delft, The Netherlands

12 ³Tigray Agricultural Research Institute, P.O. Box 492, Mekelle, Ethiopia

14 ⁴Hydraulic Research Center, P.O. Box 318, Wad Medani, Sudan

16 ⁵Mekelle University, P.O. Box 231, Mekelle, Ethiopia

18 *Correspondence to:* T.G. Gebremicael (t.gebremicael@un-ihe.org/dutg2006@gmail.com)

20 Abstract

22 Satellite rainfall products are considered important options for acquiring rainfall estimates in
24 the absence of ground measurements. However, estimates from these products need to be
26 validated as their accuracy can be affected by geographical position, topography, and climate,
28 as well as by the algorithms used to derive rainfall from satellite measurements. Eight
30 satellite-based rainfall products (TRMM, CHIRPS, RFEv2, ARC2, PERSIANN, GPCP,
32 CMAP and CMORPH) were evaluated against ground observations over the complex
34 topography of the upper Tekeze-Atbara basin in Ethiopia. The performance was evaluated at
36 various temporal (daily, monthly, seasonal) and spatial (point, sub-basin, basin) scales over
38 the period 2002-2015.

40 Results show that CHIRPS, TRMM, and RFEv2 performed well and were able to capture the
42 rainfall measured by rain gauges. The BIAS and correlation of these products were within
44 $\pm 25\%$ and > 0.5 over different time steps. The remaining products poorly performed at daily
46 time step with higher BIAS (up to $\pm 200\%$) and lower correlation (< 0.5). CMORPH,
PERSIANN, and ARCv2 were relatively better while CMAP and GPCP performed poorly
($r < 0.4$) in all conditions. The overall performance of all products was lower in the
mountainous areas of the basin with station elevation > 2500 m.a.s.l. Compared to the
lowlands, the BIAS at highlands increased by 35% whilst the correlation dropped by 28%.

Underestimation and overestimation of rainfall dominated in the mountainous and lowland
areas, respectively. CMORPH and TRMM overestimated while the remaining products
underestimated the rainfall at all spatiotemporal scales. CMAP, ARC2, and GPCP estimates
were the most affected by large underestimation. Unlike in temporal scale, the performance of
the products did not show a uniform pattern with respect to spatial scale. Their performance
improved from point to aerial comparisons in the lowlands whereas it slightly reduced
at highland areas. Poor performance in the highlands contributed to a slightly lower
performance at basin scale compared to the pixel-to-point comparison.

Our results show that rainfall estimates from CHIRPS and TRMM have a consistently good
agreement with ground rainfall at different spatiotemporal scales in the upper Tekeze-Atbara
basin. Interpolating the sparse and unevenly distributed rain gauges over the complex terrains
however introduces unknown uncertainties with respect to the actual rainfall.

Keywords: Rainfall estimation, Satellite products, validation, Nile River Basin, Ethiopia



1. Introduction

2 Accurate information on rainfall data is necessary for many operational and research fields of
water management, hydrological applications, and agricultural forecasts (Guo & Liu, 2016;
4 Sunilkumar *et al.*, 2015). It is arguably considered as the most important driving force for any
hydrological model. Despite its importance for socioeconomic development, ground-based
6 rainfall measurements are sparse and unevenly distributed, especially in developing
countries (Behrangi *et al.*, 2011; Gebremichael *et al.*, 2014). The recommended density of
8 ground rainfall measuring network in tropical regions is one gauge per 600 - 900 km² for flat
and 100 - 250 km² for mountainous areas, respectively (WMO, 1994). However, such
10 densities are not available in most tropical regions (Taye & Willems, 2013; Worqlul *et al.*,
2014). Due to different limiting factors, including climatic conditions and human geography,
12 ground rainfall stations are sparse or do not exist at the required temporal and spatial scales
(Meng *et al.*, 2014). Recently, satellite rainfall products are considered as important
14 alternative options for acquiring rainfall estimates. These products are advantageous in terms
of temporal and spatial coverage and providing data sources in ungauged basins (Dinku *et al.*,
16 2014; Katsanos *et al.*, 2016).

18 Satellite rainfall products are increasingly available with almost global coverage and the
supply of those products are becoming cost effective sources for hydrological applications
20 (Menget *et al.*, 2014; Thiemiig *et al.*, 2012). The spatiotemporal resolutions and measurement
accuracy of these products are continuously improving because of advancement in sensor
22 technologies and estimation techniques. A number of higher resolution rainfall products are
now available at a quasi-global scale (Behrangi *et al.*, 2011; Jiang *et al.*, 2012). The Tropical
24 Rainfall Measurement Mission (TRMM), African Rainfall Estimation (RFE), African Rainfall
Climatology (ARC), Global Precipitation Climatology Project (GPCP), Precipitation
26 Estimation from Remotely Sensed Information using Artificial Neural Networks
(PERSIANN) Climate Hazards Group InfraRed Precipitation with Stations (CHIRPS) and
28 CPC Morphic technique (CMORPH) are among the common products that have been widely
applied.

30
32 However, satellite rainfall products need to be validated as their accuracy can be affected by
geographical position, topography, and climate, as well as by the algorithms used to derive
rainfall from satellite measurements (Meng *et al.*, 2014; Xue *et al.*, 2013). Several studies on
34 the validation and comparisons of these products with ground measurements have been



conducted at different scales (e.g. Dinku *et al.*, 2007; Feidas, 2010; Guo & Liu, 2016;
2 Hessels, 2015; Hu *et al.*, 2014; Jiang *et al.*, 2012; Thiemig *et al.*, 2012; Worqlul *et al.*, 2014).
Nevertheless, the performance varies among the rainfall products because of different data
4 sources and retrieving algorithms (Derin & Yilmaz, 2014; Toté *et al.*, 2015). In addition, the
performance also varies for the same data type across different regions and seasons
6 (Gebremichael *et al.*, 2014; Hu *et al.*, 2014). This indicates that the performance of satellite
products largely depends on the location, topography, season, and hydro-climatic
8 characteristics of the study area. Therefore, the reliability of satellite rainfall needs to be
validated and compared against ground measurements to a specific area and temporal scales
10 before it can be used in any subsequent application (Feidas, 2010; Ouma *et al.*, 2012).

12 Validation and inter-comparison of different rainfall products over the complex topography of
the upper Tekeze-Atbara (T-A) basin are essential to determine which product is
14 representative. A number of studies have been conducted in Ethiopia to evaluate different
satellite rainfall products (e.g., Dinku *et al.*, 2007; Gebremichael *et al.*, 2014; Haile *et al.*,
16 2013; Worqlul *et al.*, 2014; Beyissa *et al.*, 2017). However, these studies have mainly
focused on the Upper Blue Nile basin and to some extent on central Ethiopia. In the T-A
18 basin, where these products can contribute to better understanding of catchment response to
land degradation and environmental rehabilitation programs, there has been no
20 comprehensive validation studies. Therefore, this study was intended to validate eight of the
widely used satellite rainfall products on different spatiotemporal scales. The relationships
22 between satellite rainfall products and topography were also carefully explored in order to
understand possible errors produced by the rugged terrains.

24

2. Study area and Data

2.1. Study area

This study was conducted in the Upper T-A basin, one of the main tributaries to the Nile river
28 located in the Northern Ethiopia, with a total catchment area of 45,694 km² at the outlet. It is
situated between 37.5° – 39.8° E and 11.5° – 14.3° N (Fig.1). The basin is characterized by
30 rugged topography with a significant variation ranging from 833 to 4530 m.a.s.l. About 0.2%,
52%, 42% and 0.62% of the land is found below 1000, between 1000-2000, 2000-3000, 3000-
32 4000 and above 4000 m.a.s.l, respectively. This clearly indicates that topography is a key
factor in influencing microclimates in the basin.



2 Figure 1: Location map and distribution of rainfall stations in the Upper T-A Basin

3 The basin is characterized by a semi-arid climate in the east and north and partly semi-humid
4 in the south (Belete, 2007). More than 85 % of the total annual rainfall falls in the wet season
5 (June -September) which varies from 400 mm yr⁻¹ in the east to more than 1200 mm yr⁻¹ in
6 the south (Fig. 2a). The variations are mainly associated with the seasonal migration of the
7 inter-tropical convergence zone (ITCZ). The beginning and ending of the ITCZ over highlands
8 of Ethiopia varies annually, which mostly causes the inter-annual rainfall variability
9 (Selshi&Zanke, 2004;Nyssen *et al.*, 2005).

10

11 The general pattern of rainfall over the basin is also modified by the complex topography
12 (Dinku *et al.*, 2007; Viste & Sorteberg, 2013). This implies that the movement of air moisture is
13 substantially modified to create contrasting rainfall regimes in the region (Huber *et al.*, 2006).
14 The sudden changes in elevation can obstruct the air mass movement to create a microclimate
15 at the bottom of mountains or can updraft over the mountains to create orographic rainfall
16 (Dinku *et al.*, 2007).

17 In most regions, rainfall increases with elevation due to the orographic uplifts (Moreno *et al.*,
18 2014;worqlul *et al.*, 2014). However, this relationship is not uniform in the T-A Basin
19 (Fig.2b). Rainfall in the mountains is higher in some areas and lower in others (Kiros *et al.*,
20 2015). Figure 2a indicates that the total annual rainfall increases with elevation in the
21 southern and southwestern parts of the basin only. In contrast, it reduces with elevation in
22 most other parts of the basin. Stations located in the highlands of the eastern and northern parts
23 of the basin receive less rainfall compared to the associated lowlands (Fig. 2a). This is
24 attributed to the complex local topography, which alters proximity to the sources of moist air
25 and seasonal movements of the ITCZ (Van der Ent *et al.*, 2010; Kiros *et al.*, 2016).

26
27 During the rainy season, the ITCZ moves towards the Northern part of the basin, which brings
28 moisture from the Atlantic and Indian oceans through westerly (Degefu *et al.*, 2016;
29 Mohamed *et al.*, 2005). When the rain-bearing winds reach the basin, their direction is
30 modified by the local topography forcing the release of moisture in the lower areas before
31 they reach the top of mountains. This creates more intense and shorter duration convective
32 rainfall events in the lowlands where warm and moist airflows encounter the mountain
33 foothill. Van der Ent *et al.* (2010) showed that topography can play an important role in
34



moisture cycling either by blocking or capturing moving air masses. Another possible reason
2 for the low rainfall over the northern-eastern highlands is that whereas here the eastern rain-
bearing winds are stronger, they carry less water vapour (Viste & Sorteberg, 2013). The non-
4 uniform patterns of rainfall against the topography can strongly influence the performance of
satellite rainfall estimates (Haile *et al.*, 2013).

6

Figure 2: Relationship between rainfall and elevation in the T-A basin

8

2.2. Datasets

10

2.2.1. Rain gauge data

Ground rainfall data used for validation of the satellite products comprised of 34 stations
12 located within and surrounding the basin (Fig.1). These data were provided by the Ethiopian
Meteorological Service Agency (NMA). The datasets cover daily data for the period from
14 2002 to 2015. Although the number of stations is relatively good, their distribution over the
basin is not uniform. Most of the gauges are located in easily accessible areas and the
16 distribution of gauges in the lowland areas are sparse (Fig. 1). Interestingly, most of the
rainfall stations with a relatively good quality of data are located in the highland areas where
18 the spatial variability of rainfall is very high. A summary of these ground measurements with
vertical locations is given as an electronic supplementary file (Table S1).

20

Quality control of rainfall data from each station was done to identify if there were outliers
22 and missing values. All outliers were then compared to neighbouring gauges to cross-check if
observed extreme values resulted from extreme climate events. Stations with large data gaps
24 in between the selected validation period were excluded from the analysis. After data
screening, 34 stations out of the 75 in the basin were found to be reliable with a relatively
26 consistent record.

2.2.2. Satellite rainfall products

28 The validation and inter-comparison of eight satellite rainfall products were performed
at daily, monthly, and seasonal scales. Table 1 provides the summary of satellite rainfall
30 products used for this study. These products were selected based on their public domain and
long-term data available, spatiotemporal resolution, near-real-time availability and their
32 common applications in Africa (Dembélé & Zwart, 2016; Dinku *et al.*, 2007; Thiemi *et al.*,
2012).



2 Table 1: Summary of selected satellite rainfall products for this study (in descending order of spatial resolution)

4 The CHIRPS datasets, developed by the US Geological Survey (USGS) and the Climate Hazards Group at the University of California are blended products which combine global climatologies, satellite observations and in-situ rainfall observations from Global Telecommunications system (GTS) (Funk *et al.*, 2014; Knapp *et al.*, 2011). CHIRPS incorporates 0.05° resolution satellite rainfall estimates with in-situ station data to produce daily time series (Katsanos *et al.*, 2016).

10

12 ARCV2 is produced by the National Oceanographic and Atmospheric Administration Climate Prediction Center (NOAA-CPC) and provides daily rainfall data over Africa. It is very similar to RFEv2 except the 30 minutes is replaced by the 3-hourly IR data (Love *et al.*, 2004).

14

16 The RFEv2 is also provided by NOAA-CPC for Famine Early Warning Systems Network to assist in disaster-monitoring activities over Africa (Herman *et al.*, 1997). RFEv2 has been operational since 2001 and uses rainfall estimates from PM sensors, IR data from METEOSAT and daily rainfall from the GTS reports. Daily rainfall estimates were obtained at 0.1° spatial resolution by merging these sources.

20

22 The CMORPH product that produces global rainfall analysis at a very high spatial and temporal resolution is also a product from NOAA-CPC. Unlike the other products, the CMORPH product is not an algorithm for merging of the PM and IR estimates rather it uses the IR information for the spatial and temporal evolution of clouds, not the rainfall estimates (Asadullah *et al.*, 2008; Joyce *et al.*, 2004). It uses rainfall estimates derived from low orbit PM observations and propagate these features using a high temporal and spatial resolution IR data (Joyce *et al.*, 2004). According to Dinku *et al.* (2007), the CMORPH combines the superior retrieval accuracy of the PM and higher resolution of IR data. This method is highly flexible as it allows incorporation of any rainfall estimate from PM satellites.

30

32 The PERSIANN precipitation estimates were developed by the Center for Hydrometeorology and remote sensing at the University of California (Ashouri *et al.*, 2015). It uses an artificial neural network approach to merging the IR and PM data and the rainfall estimates are based on the infrared brightness temperature image provided by geostationary satellites (Hsu *et al.*,

34



1997). The rainfall estimates in PERSIANN algorithm are available at 0.25° spatial
2 resolution.

4 The latest version of TRMM product (3B42V7) was developed by the National Aeronautics
and Space Administration (NASA). This product was obtained from the TRMM Multi-
6 satellite precipitation analysis (TMPA) algorithm which combines Infrared (IR) and Passive
Microwave (PM) data retrievals (Guo & Liu, 2016; Huffman *et al.*, 2007). TRMM rainfall
8 estimates incorporates gauge data for bias correction from several sources including national
and regional meteorological services. (Funk *et al.*, 2014). The TRMM3B43 rainfall products
10 were aggregated from the TRMM3B42 3-hourly estimates and merged with station data to
produce daily rainfall (Dinku *et al.*, 2007).

12

The GPCP is a blended product which combines the Global Precipitation Climatology Center
14 (GPCC) gauge data with the PM and IR rainfall estimates (Huffman *et al.*, 1997). The PM
estimates in this product are based on the Special Sensor Microwave Imager (SSM/I) data
16 from the Defence Meteorological Satellite program (DMSP, US) while the IR data came
mainly from Geostationary Operational Environmental Satellite (GOES) Precipitation Index
18 (PI) (Xie & Arkin, 1995). This technique is advantageous as it combines rainfall estimate
information from many data sources by taking the strength of each data type.

20

CMAP products include monthly and pentad (5-day) mean rainfall estimates at 2.5° spatial
22 resolution (Feidas, 2010). These techniques produce rainfall estimates by merging ground
station data with rainfall estimates from several satellite-based algorithms (Xie & Arkin,
24 1997). As described in Xie and Arkin (1997), inputs are derived by combining of
geostationary and polar orbiting infrared, PM retrievals and rain gauge observations. First, the
26 IR and PM rain estimates are merged using a maximum likelihood approach where the
estimate with weights are derived by comparison to the gauge analysis. Then, the gauge
28 analysis is used to obtain an absolute value of the merged product (Feidas, 2010).

30 **3. Methodology**

3.1. Validation processes

32 The spatial patterns of eight satellite products were evaluated and compared with rain gauge
data at daily, monthly, and seasonal scales. Both the satellite and gauge rainfall data were



collected at different temporal scale and first, the daily data were aggregated to monthly and
2 seasonal scales. As more than 85% of the total annual rainfall occurs during the wet season
(June-September) (Gebremicael *et al.*, 2017), seasonal comparison was considered only for
4 this period. The ability to replicate the observed rainfall by the products was done during this
common period between all satellite and station rainfall. Considering the given climatic
6 variability, complex topographical characteristics and hydrological working units of the basin,
the performance of these products were evaluated using two approaches, namely point-to-
8 pixel and aerial averaged rainfall comparison.

10 Rainfall over a complex topography like the T-A basin is largely subjected to small-scale
variability, which implies that evaluation of such satellite products should be at the smallest
12 possible spatial and temporal scales (Thiemig *et al.*, 2012). Accordingly, in the first approach
all satellite rainfall products from the corresponding grid cell were compared to the ground
14 observed data within the satellite box. The variance of satellite estimate is smoother in space
and time as these products are represented by the spatial averages over the pixels. For this
16 analysis, the satellite rainfall products were extracted for the location of each rainfall station
and their performance were evaluated using statistical indices. It was assumed that the amount
18 of point rainfall is uniform in the area of the pixel which may not necessarily true. The second
approach was based on the aerial rainfall comparison at different spatial scales.
20 Representative sub-basins from lowland and highland areas (Fig.1) with an average elevation
of 1400 and 3000 m.a.s.l. were considered in order to account for the effect of topography.
22 Satellite products were validated at sub-basin and basin level by comparing spatially
aggregated pixel values against a corresponding interpolated observed rainfall from gauge
24 stations using the inverse distance weighting (IDW) method (Ruelland *et al.*, 2008).

26 **3.2. Evaluation statistics**

The satellite rainfall products were quantitatively evaluated against ground observations using
28 four statistical indices: the relative percent of bias (PBIAS), Pearson correlation coefficient (r),
Root Mean Square Error (RMSE), and Mean Absolute Error (MAE) Table 2). A detailed
30 description of these indices can be found in Toté *et al.* (2015) and Thiemig *et al.* (2012).

Table 2: Statistical indices used for the satellite rainfall products performance evaluation

32

Where x_i is observed rainfall from raingauge, y_i is satellite rainfall product, N is the number of pairs of products,
34 \bar{x} and \bar{y} are the average of observed and satellite rainfall data, respectively.



2 Agreement between estimates and observation is considered satisfactory for PBIAS and r
values $\pm 25\%$ and > 0.5 , respectively (Moriassi *et al.*, 2007). The lower the RMSE and MAE
4 values, the closer the satellite estimates are to the ground measurements. The unit of RMSE
and MAE is mm/time period.

6 **4. Results and discussion**

4.1. Comparison at pixel-to-point spatial scale

8 The performance of satellite estimates was evaluated by comparing these data for 34 rainfall
stations at grid level covering the location of the station. Comparisons were carried out at
10 daily, monthly, and seasonal periods. First, daily rainfall of eight products was compared with
the observed daily rainfall. Figure 3 shows the PBIAS (%) and correlation (r) of all satellite
12 estimates against ground station values. The daily estimates performed poorly in the majority
of stations. However, CHIRPS, RFEv2 and TRMM had a relatively good performance with
14 lower PBIAS, RMSE and MAE and higher r compared to other products (Fig.3 and Tables S2-
and S3). The average value of PBIAS for all stations were -13%, -16% and 17% for CHIRPS,
16 RFEv2 and TRMM, respectively. Similarly, r value of these products was ≥ 0.5 in the majority
of stations with an average value of 0.52, 0.50 and 0.50, respectively. The RMSE and
18 MAE, which evaluates the average magnitude error between satellite estimates and ground
stations showed the same trend as PBIAS and r (Tables S2 and S3). The remaining products
20 failed to capture the observed daily rainfall with correlation of < 0.5 and higher PBIAS, RMSE
and MAE in most stations (Tables S2 and S3). The ARC2, GPCP and CMAP performed
22 poorly.

24 The precision of these products to reproduce the observed rainfall was further investigated at
monthly time series. Table 3 shows the average value of accuracy indicators obtained by
26 comparing each product with ground stations. The results indicate that the performance of all
products improved when daily data are aggregated to monthly data. The correlation for
28 CHIRPS, RFEv2 and TRMM were > 0.5 in all stations with an average value of 0.61, 0.59 and
0.56, respectively (Table 3). Similarly, the PBIAS value reduced at monthly time scale. The
30 RMSE and MAE indices also decreased at monthly scale, which implies the agreement
between satellite and ground rainfall increased (Table 3). For example, Fig. 4 compares the
32 pattern of statistical indices for all products in four representative (highland, lowland and



medium) stations. CHIRPS, RFEv2 and TRMM outperformed to the other products. ARCV2,
2 CMAP and GPCP again performed poorly with a $r < 0.5$ and higher PBIAS (Table 3).

4 Figure 3: Comparison of daily satellite rainfall estimate with ground measurements, (a)
PBIAS, (b) Correlation (r)

6

Table 3: Average accuracy indicators obtained from monthly comparison

8

Moreover, comparisons based on average monthly point rainfall (2002-2015) at the given
10 locations indicate that rainfall estimates of CHIRPS, RFEv2 and TRMM products agree with
the corresponding ground measurements (Fig.5). Monthly rainfall patterns from these
12 products have a consistent and strong agreement with the ground rainfall compared to the
remaining products.

14

To gain further information on the seasonal variations of rainfall estimate skills of the satellite
16 products, comparisons were also made for the entire rainy season (June-September). Figure 6
presents an inter-comparison of wet season rainfall estimates with the observed rainfall of the
18 same period. The spatial distribution of correlation coefficients (Fig. 6) and PBIAS (Fig.S1)
show patterns that are similar to these of the daily and monthly results. However, the
20 performance of all products was significantly improved during the wet season. Six satellite
products had an excellent agreement with ground rainfall (CHIRPS, TRMM, PERSIANN,
22 RFEv2, ARC2, and CMORPH) during the wet season. CHIRPS, RFEv2, and TRMM
correlated best with the observed rainfall compared to the remaining products. With average
24 values of 0.84, 0.74, and 0.75 for CHIRPS, RFEv2, and TRMM, respectively, the correlation
coefficient of these products showed a strong agreement. The PBIAS of these products was
26 also within the range of $\pm 25\%$ in most stations. The RMSE and MAE indices were also lower
than the other products (Tables S4 and S5). Next, the PERSIANN, CMORPH and ARCV2
28 products showed a good agreement with the gauged rainfall. Improved correlation ($r > 0.5$) and
lower PBIAS, RMSE and MAE were obtained in 80 % of the stations, however the GPCP and
30 CMAP products continued to show poor agreement despite some improvements (Fig. 6 and
Tables S4 and S5).

32

Figure 4: Monthly statistical indices at pixel to point rainfall comparison.



2 Fig 5: Comparison of mean monthly rainfall (2002-20015) at four representative
4 ground stations

6 Point-to-pixel comparison of the different temporal scales showed that all satellite products
8 suffer from both over and underestimations, explained by negative and positive values of
10 PBIAS. Both phenomena were observed in all products at several locations and time
12 scales. TRMM and CMORPH systematically overestimate the rainfall in more than 20 stations
14 while they underestimate rainfall in the remaining stations. The RFEv2, GPCP, ARC2 and
16 CMAP products consistently underestimate rainfall in the majority of ground stations. Most
18 overestimations (underestimations) were observed during the dry (October-May) (wet (June-
20 September)) months (Fig.5). However, the performance of all products to capture the
22 observed rainfall were better in the dry months. This is due to the reduced probability of
24 rainfall during the dry months.

26 Figure 6: Spatial distribution of correlation coefficients (r) during the wet season comparison.

28 It is also important to remark that inconsistent estimation of rainfall by all products is likely
30 due to the effect of rugged terrains. The overall performance of the satellite rainfall products is
32 lower in the peripheries of the basin where most stations are located in the mountainous area
 with an elevation $> 2,500$ m.a.s.l. (Fig.7). As shown in Fig. 4, lower correlation and higher
 PBIAS is observed in Debark compared to Sekota with an elevation of 3,000 and 1,960
 m.a.s.l., respectively. A relatively better performance occurred in central, eastern, and north-
 western parts of the basin where stations are located below 2,500 m.a.s.l. As an example, the
 long-term annual observed and satellite rainfall from CHIRPS were plotted against elevation
 of stations (Fig.7). The graph clearly shows that the relationship pattern of rainfall with
 elevation is not straightforward. The correlation of these products showed a poor agreement at
 higher elevation. A similar study in the neighbouring Upper Blue Nile basin by
 Gebremichael *et al.* (2014) also showed that satellite products failed to capture the ground
 rainfall in mountainous compared to lowland areas. This result is consistent with other studies
 carried out elsewhere (e.g. Asadullah *et al.*, 2008; Derin & Yilmaz, 2014; Guo & Liu, 2016;
 Hu *et al.*, 2014)



Figure 7: Relation between annual average rainfall (gauged and CHIRPS) and
elevation

2

In summary, the combination of daily, monthly, and seasonal point comparisons demonstrate
that the CHIRPS, RFEv2, TRMM, and PERSIANN products have the best agreement with the
observed rainfall across the basin. The evaluation indices at different time scales and average
monthly plots comparison show that CHIRPS performs best, followed by RFEv2 and TRMM.
Over- and under-estimation of daily, monthly and seasonal rainfall by CHIRPS was smaller
compared to the other products.

8

4.2. Comparison based on aerial averaged rainfall

Spatiotemporally aggregated aerial rainfall of each product was also compared with the
corresponding interpolated rainfall from the gauges at daily, monthly and seasonal time scales.
Table 4 shows the performance of all products at basin level and different time scale. Similar
to the point-to-pixel comparison, the CHIRPS, RFEv2, TRMM, PERSIANN, and CMORPH
aerial rainfall estimates had the best accuracy, with PBIAS within $\pm 25\%$ at all temporal scales.
However, all products showed a lower performance in terms of correlation with < 0.5 and
higher RMSE and MAE at daily compared to monthly and seasonal time scales. Lower
performance at daily scale can be explained by erroneous (non-detection) of more localized
convective rainfall events. The CMAP, ARCV2, and GPCP continued to show lower r and
higher RMSE, MAE and PBIAS consistently at all time scales. The performance improved at
monthly and seasonal scales (Table 4). Higher accuracies at larger time scales are due to the
fact that the errors at smaller time scale are symmetrical and offset each other when
aggregated.

22

The negative and positive values of PBIAS in Table 4 confirms that most products
underestimated rainfall during the wet season, except TRMM and CMORPH. Figure 8 shows
the visual comparison of the long-term monthly aerial average of satellite estimates with the
corresponding ground aerial rainfall. It clearly indicates that the TRMM and CMORPH
products consistently overestimated, whereas CMAP, GPCP and ARC2 underestimated
rainfall in all months. The remaining products showed a varied picture for the different
months. For example, CHIRPS and RFEv2 slightly underestimated rainfall during the rainy
months of July and August whilst overestimating rainfall in the dry months (Fig. 8). During the
wet season CHIRPS satellite estimates outperformed the other products.

32



Table 4: Comparison of satellite and observed aerial rainfall, at basin scale, at different time scales

2

Figure 8: Monthly average satellite estimates and ground rainfall comparison at basin scale

4 Whereas all satellite rainfall estimates showed a consistent improving pattern with increasing
time scale, their performance did not show a uniform pattern with increasing spatial
6 scale. Figure 9 shows a comparison of the average correlation of the products at different spatial scales
for the wet season. Most products performed worse at basin scale compared to pixel-to-point
8 and lowland sub-basin scales. The likely reason is that the aerial averaged rainfall over the
complex topography suffers from limitations due to the uneven distribution of rain gauges.
10 The performance of CHIRPS, TRMM, and CMAP improved at basin level compared to pixel-
to-point scale whilst all other products performed worse (Fig. 9). The relatively poor
12 performance at the basin scale for most products is likely due to the topographical variations
across the basin. Variations of topography can significantly compromise the interpolation of
14 observed rainfall (Thiemig *et al.*, 2012). The rainfall stations are also sparsely and unevenly
distributed over the basin, which can be a source of systematic errors when interpolating
16 aerial rainfall (Dembélé & Zwart, 2016; Toté *et al.*, 2015).

18 To further understand the effect of complex terrains on the performance of the satellite
products, the seasonal aerial rainfall of representative highland and lowland sub-basins was
20 compared (Fig. 9). The result of the two contrasting topographic features demonstrates that
the overall correlation of satellite rainfall estimates is better in lowland than in high
22 mountainous areas. This suggests that the satellite products may not accurately capture the
spatial pattern of seasonal rainfall in complex topographic areas like the T-A basin. Further,
24 all products overestimate rainfall in the lowlands and underestimate rainfall of the rain in the
highlands. However, comparing both topographic features, the magnitude of underestimation
26 was greater than that of overestimation in most products. For example, CHIRPS, TRMM, and
CMORPH underestimated the wet season rainfall over the highland area by 32, 28, and 52%,
28 while it overestimated by 18, 21, and 28% the lowland rainfall, respectively.

30 Fig. 9: Comparison of seasonal averaged correlation at a pixel, sub-basin, and basin scales

32 In summary, based on the comprehensive evaluation at different temporal and spatial scales,
the CHIRPS, RFEv2, and TRMM outperformed the other satellite rainfall products at all



spatiotemporal scales. The better performance of CHIRPS can be explained by the fact that it
2 to considers topographic effects and its high spatial resolution (Katsanos *et al.*, 2016). The
good performance of TRMM, and RFEv2 is possibly due to the fact that these products have a
4 bias correction that is based on rain gauge data (Thiemig *et al.*, 2012).

6 Our findings are in agreement with similar studies (e.g. Dembélé & Zwart, 2016; Hessels,
2015; Katsanos *et al.*, 2016; Bayissa *et al.*, 2017; Dinku *et al.*, 2008). Hessels (2015)
8 compared 10 satellite products over the Nile basin and CHIRPS and TRMM were found to be
the best-performing products. Bayissa *et al.* (2017) revealed that CHIRPS estimates showed
10 better performance than PERSIAN and TARCAT over the Upper Blue Nile basin. Similarly,
Gebremichael *et al.* (2014) and Dinku *et al.* (2007) showed that CMORPH and TRMM well
12 performed in the rugged terrains of neighbouring basins. Next to these products, CMORPH,
PERSIANN, and ARCV2 were better in capturing the observed rainfall while CMAP and
14 GPCP poorly performed at all spatiotemporal scales. Dinku *et al.* (2007) also showed that
CMAP and GPCP products poorly performed compared to TRMM and CMORPH in
16 Ethiopia.

18 The performance of all products consistently correlated best with ground measurements when
aggregated at larger time scales. Improved performance with increasing time step is obviously
20 due to counterbalancing of variabilities when accumulated from smaller to larger time scales.
Many studies (e.g. Dembele & Zwart, 2016; Guo & Liu, 2016; Meng *et al.*, 2014) reported that
22 the performance of satellite estimates improved as time step increased. In contrast, the
performance of these products was not uniform with an increasing spatial scale. The
24 performance of all products increased from point rainfall to aerial rainfall in the lowlands,
whereas their performance decreased in the highlands (Fig. 9). A poorer performance in the
26 mountainous area is notable for all products. This result is in agreement with other studies
(e.g. Derin and Yilmaz; 2014; Dinku *et al.*, 2007) which indicates that satellite rainfall products
28 have challenges to estimate orographic precipitation in basins with a complex topography.

5. Conclusions and Recommendations

30 This study evaluated the performance of eight-satellite based rainfall products ranging from
high to low resolution over the T-A basin. These products were evaluated and compared
32 with ground stations during 2002-2015. A comprehensive approach was applied that
included point-to-pixel and aerial averaged comparisons at different spatial and temporal scales



(daily, monthly, and seasonal). The relationship between rainfall and elevation was also analysed to identify the effects of topography on the performance.

The results showed that the CHIRPS, RFEv2, and TRMM rainfall estimates outperformed the other products consistently across all temporal and spatial scales. These products achieved acceptable correlation coefficients (>0.5) and PBIAS, RMSE and MAE values for both approaches and at all time scales. The PBIAS of these products were within $\pm 25\%$ at all time scales. CMORPH, PERSIANN, and ARC2 achieved lower scores. The performance of CMAP and GPCP was poor over the various conditions with PBIAS ranging from -250% to 118% and correlation <0.5 . A relatively lower performance is notable for all products in the mountainous areas.

The agreement between the products and rain gauge improved with increase in time scale. This is due to the fact that errors at smaller time scales offset each other when aggregated. All satellite estimates suffered from under- and over-estimation during the different time and spatial scales. Underestimation dominated in the mountainous areas. TRMM and CMORPH overestimated rainfall whilst the remaining products underestimated rainfall consistently at all spatiotemporal scales. CMAP, ARC2, and GPCP estimates were the most affected by large underestimations across all stations. Another key finding of this study is that unlike in time, the performance of the products did not show a uniform pattern at different spatial scales. The performance improved when increasing the aerial averaged rainfall in the lowlands, whereas it decreased at larger spatial scale in the highlands. Accuracy indicators at point-to-pixel comparison were slightly better than aerial averaged rainfall in the whole basin. Poor performance over the mountain areas contributed to lower performance at larger spatial scales. Moreover, systematic errors during the interpolation of observed rainfall over the complex topography of the basin might have contributed to the overall lower performance at the basin scale.

The ranking of these products may not be absolute as validation of these products in different study periods could result in different rankings. Interpolation of the sparse and unevenly distributed rain gauges over complex terrain may also introduce significant uncertainties and therefore limits the validity of the result. However, considering the current data availability, the result of this study provides a basis for the utilization of satellite rainfall estimates over the complex topography of the T-A basin. It will be a good reference for future applications of satellite rainfall, especially in rain gauge sparse and ungauged basins with rugged terrains.



2 **Acknowledgement:** This study was carried out with the support of the Netherland Fellowship
Programme (NUFFIC) and the Tigray Agricultural Research Institute (TARI). The authors
4 would like to thank the Ethiopian National Meteorological Agency for providing the weather
data.

6 References

- 8 Asadullah, A., McIntyre, N., & Kigobe, M.: Evaluation of five satellite products for estimation of
rainfall over Uganda. *Hydrolog. Sci. J.*, 53(6), 1137-1150, 2008.
- 10 Ashouri, H., Hsu, S., Sorooshian, D., Braithwaite, K., Knapp, D., Cecil, B. Prat, C.: PERSIANN-
CDR: Daily Precipitation Climate Data Record from Multisatellite Observations for
Hydrological and Climate Studies. *B. Amr. Meteor. Soc.*, 96(1), 69-83, 2015.
- 12 Bayissa, Y., Tadesse, T., Demisse, G., & Shiferaw, A.: Evaluation of Satellite-Based Rainfall
Estimates and Application to Monitor Meteorological Drought for the Upper Blue Nile Basin,
Ethiopia. *Remote Sens.*, 9(7), 669, 2017.
- 14 Behrangi, A., Behnaz, K., Tsou, C., Amir, A., Kuolin, S., Soroosh, S., & Bacchetta, N.: Hydrologic
evaluation of satellite precipitation products over a mid-size basin. *J. Hydrol.*, 397 225-237,
2015.
- 18 Belete, k.: Sedimentation and Sediment Handling at Dams in Tekeze River Basin, Ethiopia. (PhD
thesis), Norwegian University of Science and Technology, Trondheim, Norway, 2007.
- 20 Dembélé, M., & Zwart, S. J.: Evaluation and comparison of satellite-based rainfall products in Burkina
Faso, West Africa. *Int. J. Remote Sens.*, 37(17), 3995-4014, 2016.
- 22 Derin, Y., & Yilmaz, K. K.: Evaluation of multiple satellite-based precipitation products over complex
topography. *J. Hydrometeorol.*, 15(4), 1498-1516, 2014.
- 24 Dinku, T., Ceccato, P., Grover-Kopec, E., Lemma, M., Connor, S., & Ropelewski, C.: Validation of
satellite rainfall products over East Africa's complex topography. *Int. J. Remote Sens.*, 28(7),
26 1503-1526, 2007.
- 28 Feidas, H.: Validation of satellite rainfall products over Greece. *Theor. Appl. Climatol.*, 99, 193-216,
2010.
- 30 Funk, C. C., Peterson, P. J., Landsfeld, M. F., Pedreros, D. H., Verdin, J. P., Rowland, J. D., Verdin, A.
P.: A quasi-global precipitation time series for drought monitoring. *US Geological Survey
Data Series*, 832(4), 2014.
- 32 Gebremicael, T. G., Mohamed, Y. A., v. Zaag, P., & Hagos, E. Y.: Temporal and spatial changes of
rainfall and streamflow in the Upper Tekezē–Atbara river basin, Ethiopia. *Hydrol. Earth Syst.
34 Sci.*, 21(4), 2127-2142, 2017.
- 36 Gebremichael, M., Bitew, M. M., Hirpa, F. A., & Tesfay, G. N.: Accuracy of satellite rainfall
estimates in the Blue Nile Basin: Lowland plain versus highland mountain. *Water Resour. Re.*,
50(11), 8775-8790, 2014.
- 38 Guo, R., & Liu, Y.: Evaluation of Satellite Precipitation Products with Rain Gauge Data at Different
Scales: Implications for Hydrological Applications. *Water*, 8(7), 28, 2014.
- 40 Haile, A., Habib, E., & Rientjes, T.: Evaluation of the Climate Prediction Center (CPC) morphing
technique (CMORPH) rainfall product on hourly time scales over the source of the Blue Nile
42 River. *Hydrol. Process.*, 27(12), 1829-1839, 2013.
- 44 Herman, A., Kumar, P., Arkin, P., & Kousky, V.: Objectively Determined 10-Day African Rainfall
Estimates Created for Famine Early Warning Systems. *Int. J. Remote Sens.*, 18, 2147-2159,
1997.
- 46 Hessels, T. M.: Comparison and Validation of Several Open Access Remotely Sensed Rainfall
Products for the Nile Basin. TU Delft, Delft University of Technology, The Netherlands,
48 2015.



- 2 Hsu, K., Gao, X., Sorooshian, S., & Gupta, H.: Precipitation estimation from remotely sensed
information using artificial neural networks. *J. Appl. Met.*, 36, 1176-1190, 1997.
- 4 Hu, Q, Yang D, Li Z, Mishra A, Wang Y, & Yang H.: Multi-scale evaluation of six high-resolution
satellite monthly rainfall estimates over a humid region in China with dense rain gauges. *Int.
J. Remote Sens.*, 35(4), 2014.
- 6 Huber, U. M., Bugmann, H. K., & Reasoner, M. A.: Global change and mountain regions: an
overview of current knowledge: Springer, Dordrecht, Netherlands, 2006.
- 8 Huffman, G., Adler, F., Rudolf, B., Schneider, U., & Keehn, P.: The Global Precipitation Climatology
Project (GPCP) combined precipitation dataset. *Bull. MAEr. Meteor. Soc.*, 78, 5-20, 1997.
- 10 Huffman, G., Bolvin, D., Nelkin, E., Wolff, D., Adler, R., Gu, G., Stocker, E.: The TRMM
multisatellite precipitation analysis (TMPA): quasi-global, multiyear, combined-sensor
12 precipitation estimates at fine scales. *J. Hydrometeorol.*, 8, 38-55, 2007.
- 14 Jiang, S., Ren, L., Hong, Y., Yong, B., Yang, X., Yuan, F., & Ma, M.: Comprehensive evaluation of
multi-satellite precipitation products with a dense rain gauge network and optimally merging
16 their simulated hydrological flows using the Bayesian model averaging method. *J. Hydrol.*,
452, 213-225, 2012.
- 18 Joyce, R., Janowiak, J., Arkin, P., & Xie, P.: CMORPH: a method that produces global precipitation
estimates from passive microwave and infrared data at high spatial and temporal resolution. *J.
Hydrometeorol.*, 5, 487-503, 2004.
- 20 Katsanos, D., Retalis, A., & Michaelides, S.: Validation of a high-resolution precipitation database
(CHIRPS) over Cyprus for a 30-year period. *Atmos. Res.*, 169, 459-464, 2015.
- 22 Kiros, G., Shetty, A., & Nandagiri, L.: Analysis of variability and trends in rainfall over northern
Ethiopia. *Arab. J. Geosci.*, 9(6), 451, 2016.
- 24 Knapp, K., Ansari, S., Bain, C., Bourassa, M., Dickinson, M., Funk, C., Huffman, G.: Globally
gridded satellite observations for climate studies. *Bull. Am. Meteorol. Soc.*, 92, 893-907, 2011.
- 26 Love, T., Kumar, V., Xie, P., & Thiaw, W.: A 20-year daily Africa precipitation climatology using
satellite and gauge data. Paper presented at the Conference on Applied Climatology, 11-15
28 January 2004, Seattle, WA, 2004.
- Meng, J., Li, L., Hao, Z., Wang, J., & Shao, Q.: Suitability of TRMM satellite rainfall in driving a
30 distributed hydrological model in the source region of Yellow River. *J. Hydrol.* 509, 320-332,
2014.
- 32 Moriasi, D. N., Arnold, J. G., Van Liew, M. W., Bingner, R. L., Harmel, R. D., & Veith, T. L.: Model
evaluation guidelines for systematic quantification of accuracy in watershed simulations.
34 *TASABE.*, 50(3), 885-900, 2007.
- Moreno, J. F., Mannaerts, C. M., & Jetten, V.: Influence of topography on rainfall variability in
36 Santiago Island, Cape Verde. *Int. J. Climatol.*, 34(4), 1081-1097, 2014.
- Nyssen, J., Vandenreyken, H., Poesen, J., Moeyersons, J., Deckers, J., Haile, M., Govers, G.: Rainfall
38 erosivity and variability in the Northern Ethiopian Highlands. *J. Hydrol.*, 311, 172-187, 2005.
- Ouma, Y. O., Owiti, T., Kipkorir, E., Kibiyi, J., & Tateishi, R.: Multitemporal comparative analysis of
40 TRMM-3B42 satellite-estimated rainfall with surface gauge data at basin scales: daily,
decadal and monthly evaluations. *Int. J. Remote Sens.*, 33(24), 7662-7684, 2012.
- 42 Ruelland, D., Ardoin-Bardin, S., Billen, G., and Servat, E.: Sensitivity of a lumped and semi-
distributed hydrological model to several methods of rainfall interpolation on a large basin in
44 West Africa. *J. Hydrol.*, 361, 96-111, 2008.
- 46 Seleshi, Y., & Zanke, U.: Recent changes in rainfall and rainy days in Ethiopia. *Int. J. Climatol.*,
24(8), 973-983, 2004.
- Sunilkumar, K., Narayana Rao, T., Saikranthi, K., & Purnachandra Rao, M.: Comprehensive
48 evaluation of multisatellite precipitation estimates over India using gridded rainfall data.
J. Geophys. Res. - Atmosph., 120(17), 8987-9005, 2015.
- 50 Taye, M. T., & Willems, P.: Identifying sources of temporal variability in hydrological extremes of the
upper Blue Nile basin. *J. Hydrol.*, 499, 61-70, 2013.
- 52 Thiemi, V., Rojas, R., Zambrano-Bigiarini, M., Levizzani, V., & De Roo, A.: Validation of satellite-
based precipitation products over sparsely gauged African river basins. *J. Hydrometeorol.*,
13(6), 1760-1783, 2012.



2 Toté, C., Patricio, D., Boogaard, H., van der Wijngaart, R., Tarnavsky, E., & Funk, C.: Evaluation of
Satellite Rainfall Estimates for Drought and Flood Monitoring in Mozambique. *Remote Sens.*,
7(2), 1758, 2015.

4 Van der Ent, R. J., Savenije, H. H., Schaefli, B., & Steele-Dunne, S. C.: Origin and fate of
atmospheric moisture over continents. *Water Resour. Res.*, 46(9), W09525, 2010.

6 Viste, E., & Sorteberg, A.: Moisture Transport and Precipitation in Ethiopia. *Int. J. Climatol.*, 33(1),
249-263, 2013.

8 WMO.: World Meteorological Organization Guide to Hydrological Practices: Data Acquisition and
Processing, Analysis, Forecasting and Other Applications. Geneva, Switzerland, 1994.

10 Worqlul, A, Maathuis, B., Adem, A. A., Demissie, S. S., Langan, S., & Steenhuis, T. S.: Comparison
of rainfall estimations by TRMM 3B42, MPEG and CFSR with ground-observed data for the
12 Lake Tana basin in Ethiopia. *Hydrol. Earth Syst. Sci.*, 18(12), 4871-4881, 2014.

Xie, P., & Arkin, A.: An Intercomparison of Gauge Observations and Satellite Estimates of Monthly
14 Precipitation. *J. Appl. Meteorol.*, 34 (5), 1143-1160, 1995.

Xie, p., & Arkin, p.: Global precipitation: a 17-year monthly analysis based on gauge observations,
16 satellite estimates, and numerical model outputs. *B. Amr. Meteor. Soc.*, 78, 2539-2558, 1997.

18 Xue, X., Hong, Y., Limaye, A. S., Gourley, J. J., Huffman, G. J., Khan, S. I., Chen, S.: Statistical and
hydrological evaluation of TRMM-based Multi-satellite Precipitation Analysis over the
Wangchu Basin of Bhutan: Are the latest satellite precipitation products 3B42V7 ready for use
20 in ungauged basins? *J. Hydrol.*, 499, 91-99, 2013.

22

24

26

28

30

32

34

36

38

40

42

44

46

48

50

52



2 Table 1: Summary of selected satellite rainfall products for this study (in descending order of spatial resolution)

Product	Temporal resolution	Spatial resolution	Coverage	Starting date
CHIRPSv8	Daily	0.05°	50°N-50°S,0°-360°E	1981
ARCv2	Daily	0.1°	40°N-40°S,20°W-55°E	1983
RFEv2	Daily	0.1°	40°N-40°S,20°W-55°E	2001
CMORPH	3 hourly	0.25°	Global	2002
PERSIANN	Daily	0.25°	Global	1983
TRMM 3B42v7	Daily	0.25°	50°N-50°S,0°-360°E	1998
GPCP	Daily	1.0°	Global	1979
CMAP	pentad	2.5°	Global	1998

4

6

8

10

12

14

16

18

20

22

24

26

28 Table 2: Statistical indices used for the satellite rainfall products performance evaluation



Statistical measure	Equation	Ranges	Perfect score
Root Mean Square Error (RMSE)	$\sqrt{1/N \sum_{i=1}^n (y_i - x_i)^2}$	0 to ∞	0
Mean Absolute Error (MAE)	$1/N \sum y_i - x_i $	0 to ∞	0
Percent of bias (PBIAS)	$((\sum y_i - \sum x_i) / \sum x_i) * 100$	0 to ∞	0
Pearson correlation coefficient (r)	$\frac{\sum (x_i - \bar{x})(y_i - \bar{y})}{\sqrt{(\sum (x_i - \bar{x})^2) \sum (y_i - \bar{y})^2}}$	-1 to 1	1

2 Where x_i is observed rainfall from rain gauge, y_i is satellite rainfall product, N is the number of pairs of products, \bar{x} and \bar{y} are the average of observed and satellite rainfall data, respectively.

4

6

8

10

12

14

16

18

20

22

24

26

28



Table 3: Average accuracy indicators obtained from monthly comparison

Satellite estimate	PBIAS (%)	r	RMSE (mm/month)	MAE (mm/month)
CHIRPS	-8	0.61	17	16
ARCV2	-50	0.43	112	98
RFEv2	-10	0.56	23	21
CMORPH	14	0.48	75	29
PERSIANN	-11	0.52	41	23
TRMM	7	0.59	32	26
GPCP	-27	0.36	143	103
CMAP	-42	0.32	126	83

2

4

6

8

10

12

14

16

18

20

22

24

26



2 Table 4: Comparison of satellite and observed aerial rainfalls at basin level with different time scale

Indices	Temporal scale	CHIRPS	ARC2	RFEv2	CMORPH	PERSIANN	TRMM	GPCP	CMAP
PBIAS	Daily	<i>-10</i>	<i>-58</i>	<i>-8</i>	<i>18</i>	<i>-13</i>	<i>11</i>	<i>-41</i>	<i>-38</i>
	Monthly	<i>-8</i>	<i>-41</i>	<i>-6</i>	<i>15</i>	<i>-11</i>	<i>8</i>	<i>-28</i>	<i>-33</i>
	Wet season	<i>-6</i>	<i>-21</i>	<i>-3</i>	<i>11</i>	<i>-8</i>	<i>6</i>	<i>-19</i>	<i>-24</i>
r	Daily	<i>0.49</i>	<i>0.22</i>	<i>0.48</i>	<i>0.19</i>	<i>0.28</i>	<i>0.41</i>	<i>0.15</i>	<i>0.21</i>
	Monthly	<i>0.69</i>	<i>0.39</i>	<i>0.5</i>	<i>0.41</i>	<i>0.54</i>	<i>0.56</i>	<i>0.3</i>	<i>0.28</i>
	Wet season	<i>0.88</i>	<i>0.41</i>	<i>0.72</i>	<i>0.55</i>	<i>0.64</i>	<i>0.7</i>	<i>0.36</i>	<i>0.39</i>
RMSE (mm)	Daily	36	111	50	42	48	25	89	60
	Monthly	42	178	61	70	49	34	205	80
	Wet season	79	201	67	112	137	142	395	309
MAE (mm)	Daily	19	102	25	39	48	25	79	54
	Monthly	41	141	36	68	51	31	131	78
	Wet season	71	198	68	102	131	123	171	229

Values in italics indicate acceptable region of PBIAS (-25% - 25%) and correlation coefficient ($r > 0.5$)

4

6

8

10

12

14

16

18

20

22

24

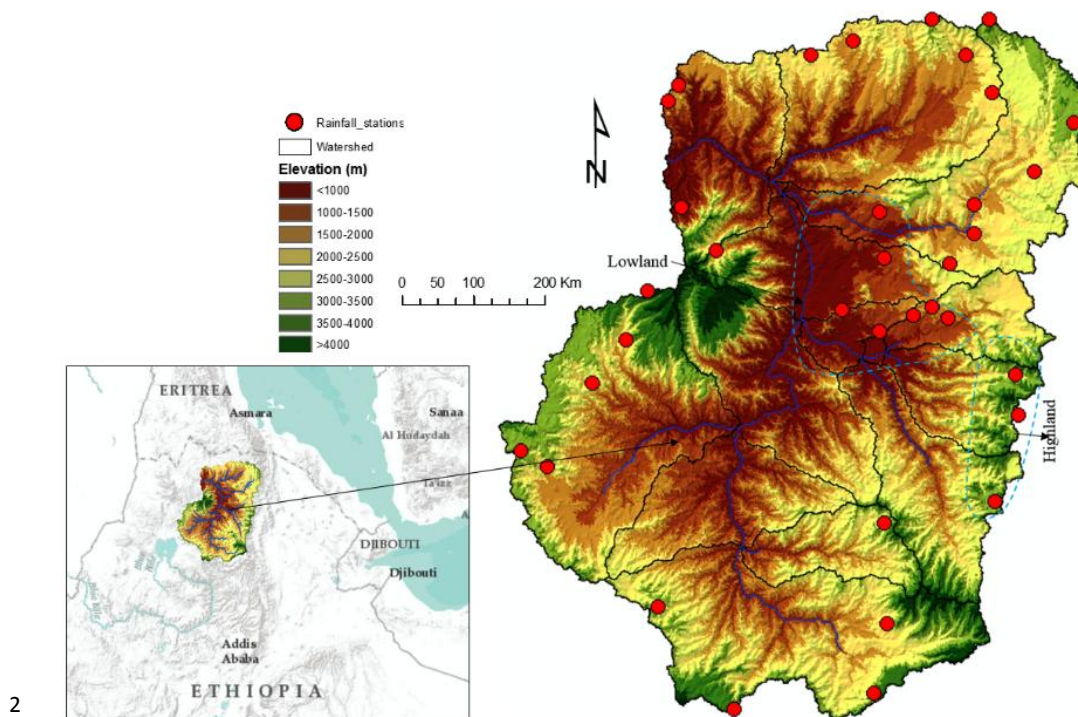


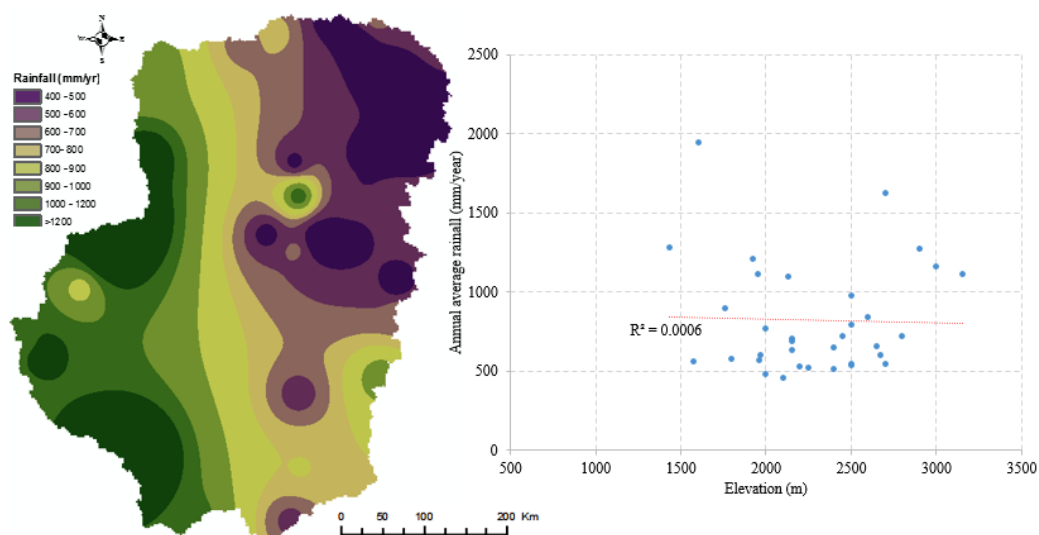
Figure 1: Location map and distribution of rainfall stations in the Upper T-A Basin



2

4

6



8

Figure 2: Relationship between rainfall and elevation in the T-A basin

10

12

14

16

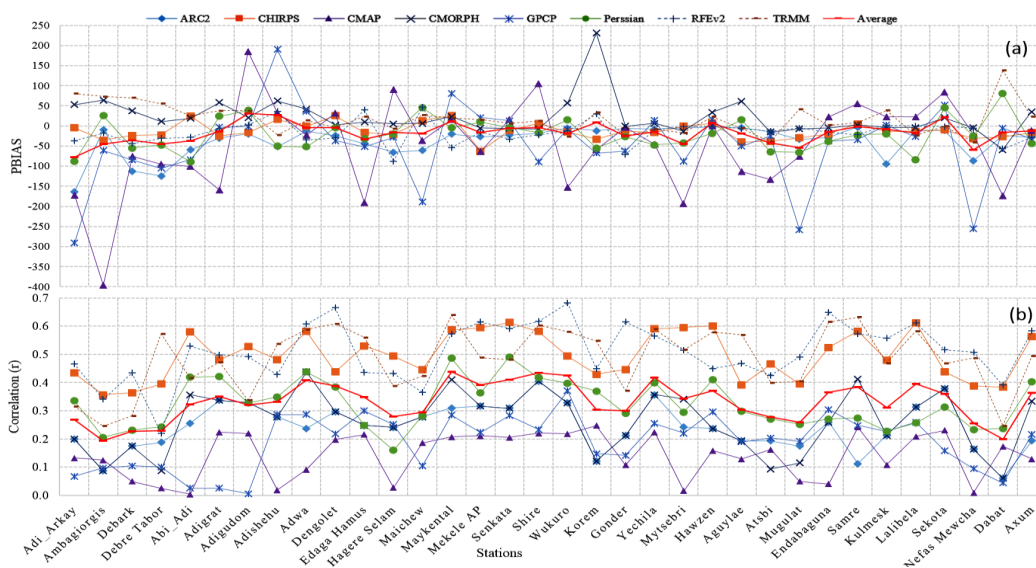
18

20

22



2
 4
 6
 8
 10

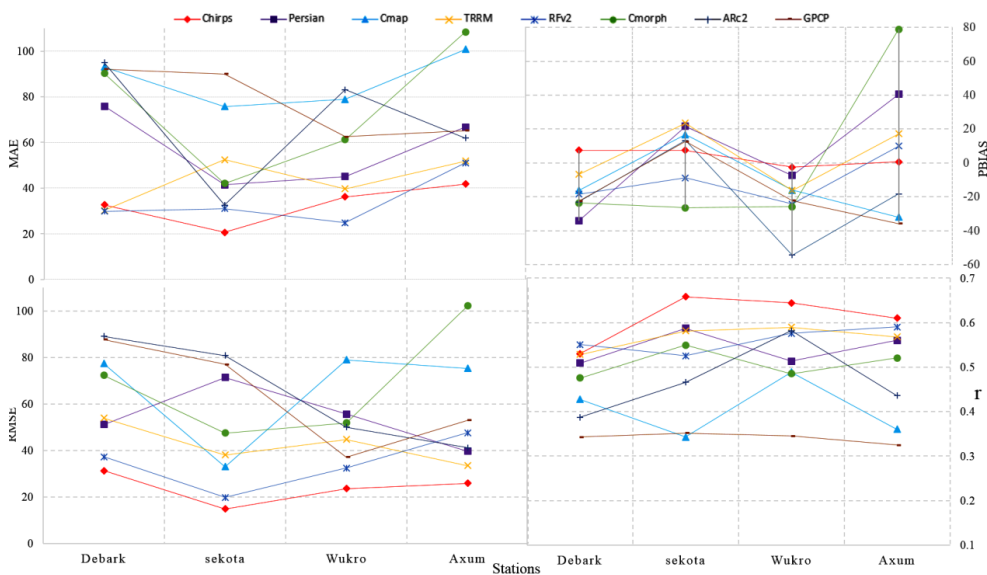


12 Figure 3: Comparison of daily Satellite rainfall estimate with ground measurements, (a)
 PBIAS, (b) Correlation (r)

14
 16
 18
 20
 22



2
 4
 6
 8
 10

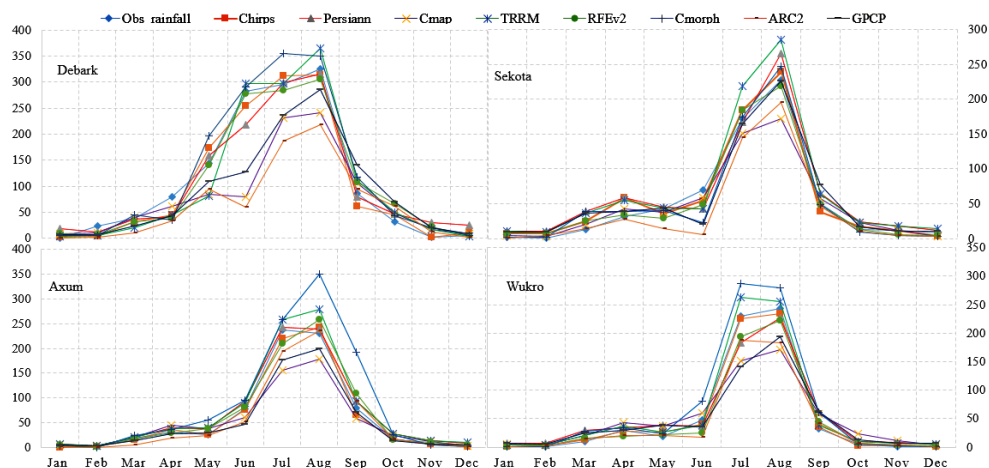


12 Figure 4: Monthly statistical indices at pixel to point rainfall comparison.

14
 16
 18
 20
 22

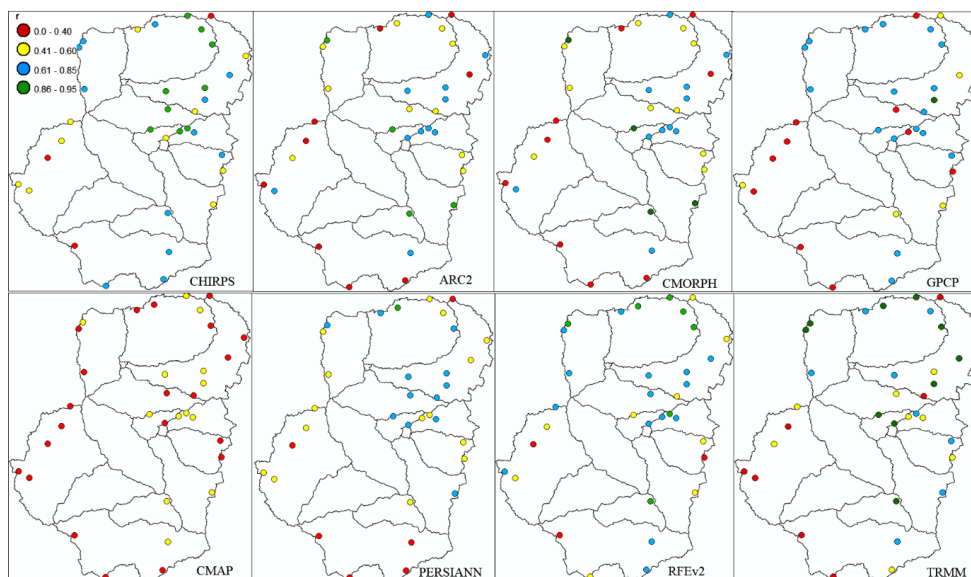


2
 4
 6
 8
 10
 12



14
 16
 18
 20
 22

Fig 5: Comparison of mean monthly rainfall (2002-20015) at four representative ground station



2 Figure 6: Spatial distribution of correlation coefficients (r) during the wet season comparison.

4

6

8

10

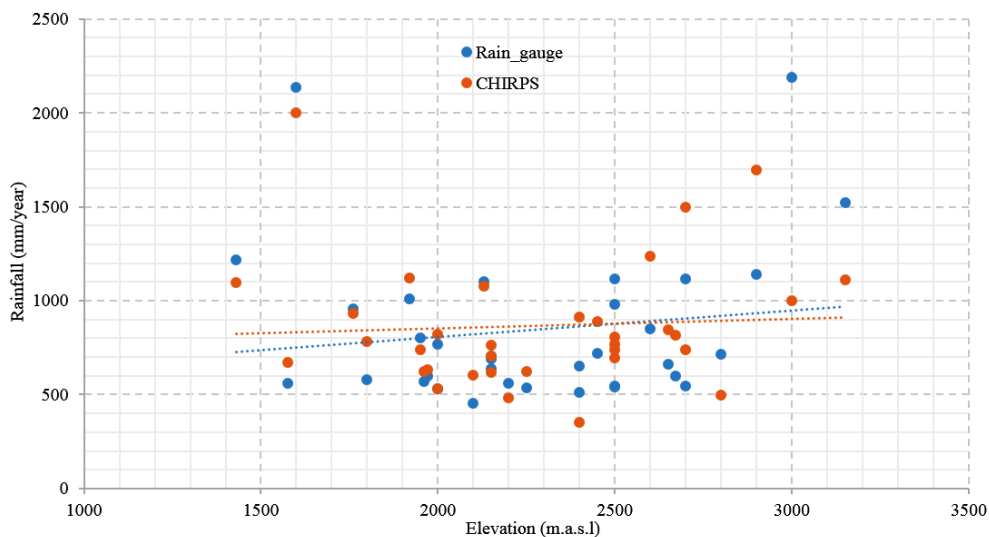
12

14

16

18

20



2 Figure 7: Comparison of annual average rainfall with elevation

4

6

8

10

12

14

16

18

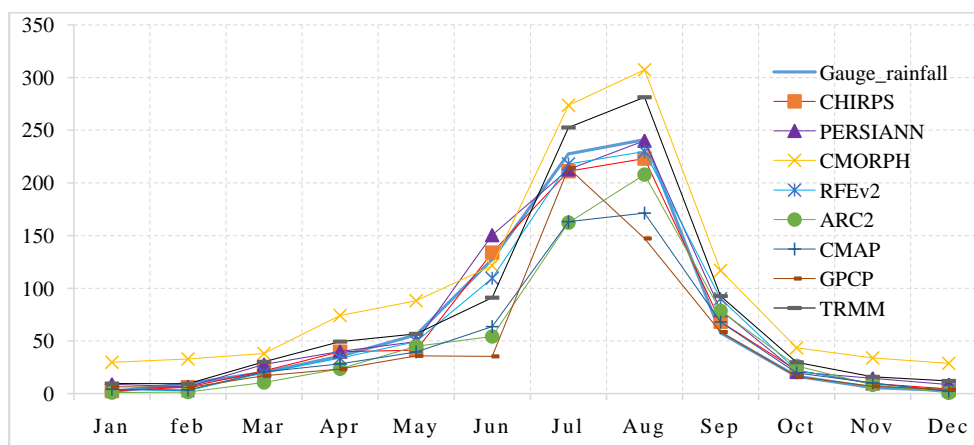
20

22



2

4



6 Figure 8: Monthly average satellite estimates and ground rainfall comparison at basin scale

8

10

12

14

16

18

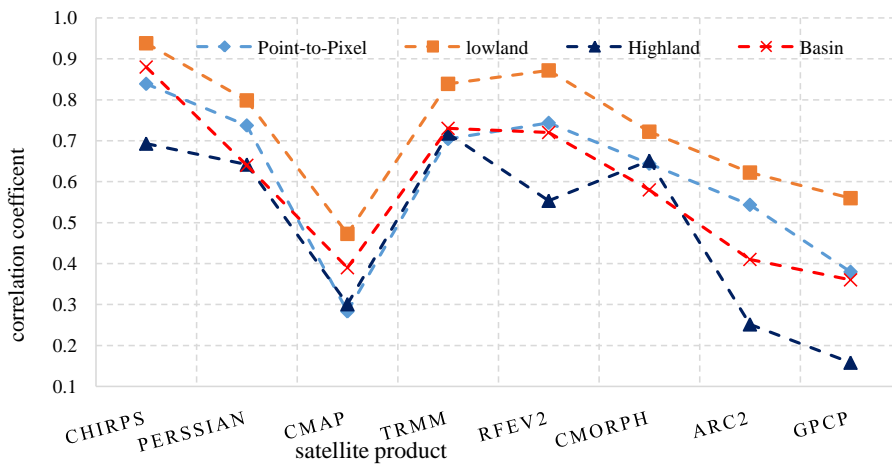
20

22

24



2



4

Fig.9: Comparison of seasonal averaged correlation at a pixel, sub-basin, and basin scales

6

8

10

12

14

16